Supporting Information:

Pt_n-$Mn^{(II)}N_x$ and Pt_n-$Mn^{(III)}N_x$ are both winning combinations for the durability of these hybrid catalysts in PEM fuel cells: A deep insight into synergism between Pt clusters and MnN_x/C sites

Vassili P. Glibin - *Department of Chemical and Biochemical Engineering, University of Western Ontario, London (Ontario), N6A 5B9, Canada;* orcid.org/0000-0003-3427-669X; Email: vassili.glibin@gmail.com

Jean-Pol Dodelet - *Institut National de la Recherche Scientifique (INRS), Centre Énergie Matériaux Télécommunications, Varennes (Québec), J3X1P7, Canada*; orcid.org/0000-0002-4978-0218; Email: jean-pol.dodelet@inrs.ca

Gaixia Zhang - *Department of Electrical Engineering, École de Technologie Supérieure (ÉTS), Montréal (Québec) H3C 1K3, Canada*; orcid.org/0000-0002-5340-8961; Email: gaixia.zhang@etsmtl.ca

S1. Number of atoms in a Pt cluster/nanoparticle, its size and its mean coordination number.

S1.1. Size of metal clusters/nanoparticles

In ref 1, the nanoparticles were considered as a dense packing of hard spheres with structures that derive from known structures of crystalline metals. The outer radius of each of these structures, R, was defined as corresponding to the smallest sphere which completely encloses the nanoparticle made up of close-packed hard spheres, each with a radius r_0, and which can be taken equal to the atomic radius of a metal. The following structures were taken into consideration for Pt: cube-octahedron (face-centered cubic lattice), truncated bipyramid (hexagonal close-packed lattice), rhombic dodecahedron (body-centered cubic lattice) and icosahedron (a slightly distorted face-centered cubic lattice). To estimate the outer radius (R) of these Pt structures, the following formulas were derived:[1]

$$R\ (\text{cube-octahedron}) \approx 1.339 r_0 n^{1/3} \quad (S1)$$

$$R\ (\text{truncated hexagonal bipyramid}) \approx 1.317 r_0 n^{1/3} \quad (S2)$$

$$R\ (\text{rhombic dodecahedron}) \approx 1.455 r_0 n^{1/3} \quad (S3)$$

$$R\ (\text{icosahedron}) \approx 1.339 r_0 n^{1/3} \quad (S4)$$

Nie et al.[2] showed, using DFT (density functional theory) calculations, that structural transitions from triangular clusters to icosahedral and face-centered cubic-like clusters occur at around n = 19 and 38, respectively. The calculations using the above formulas are close to the data obtained using the high-resolution transmission electron microscopy of the crystalline metal nanoparticles.[3] It should also be noted, that the results of the calculations by the formulas S1-S4 differ somewhat (due to the modeling of clusters' size using the ideal geometric polyhedral) from experimental data of Figure 2 in ref 4. To reconcile these values with each other, the values calculated with the

formulas S1-S4 should be multiplied by a coefficient of ~1.17. As an example, submitting n = 150 and atomic radius of platinum of 1.39 Å[5] into eq S1, one obtains R= 9.9 Å or 1.17×9.9 = 11.6 Å. It corresponds to a nanoparticle's size (2R) of 23.2 Å or ~2.3 nm.

S1.2. Mean coordination numbers of Pt atoms in the clusters/nanoparticles.

Small clusters (from n =3 to n = 10)

The mean coordination number of atoms in the cluster, $\overline{CN}$, is calculated as the quotient of the total number of pairwise nearest neighbors divided by the number of atoms, n, in a cluster.[6] Considering the geometric structure of the Pt clusters in the range of n from 4 to 10,[2] the mean coordination numbers for several small clusters (having the lowest energy structures) were calculated. These values are given in Table S1.

Table S1. Geometric mean coordination numbers of small Pt clusters

n	4	5	6	7	8	9	10
$\overline{CN}$	3	3	3	3.4	3.5	3	4.4

Large clusters (from n = 12 to n = 46)

The mean coordination numbers of clusters with n, ranging from 12 to 46, were calculated in ref 7 using the first principles Stochastic Surface Walking (SSW) global search. The statistical treatment of these values in this work gives eq S5:

$$\overline{CN} = 0.094n + 3.08 \quad \text{(S5)}$$

Nanoparticles (from n = 39 to 205)

By fitting, with a logistic regression, the data presented in Table 2 of ref 6, the following equation, describing the dependence of the mean coordination number, $\overline{CN}$, on the number atoms n, is obtained:

$$\overline{CN} = 10.29/[1 + 0.89e^{(-0.014n)}] \quad \text{(S6)}$$

Note that the logistic regression is applied for phenomena in which there is a continuous increase of one factor as another factor increases, until a saturation point is reached.

S2. Evaluation of the cohesive (binding) energy, potential of ionization, and electron affinity of Pt_n clusters/nanoparticles using Müller and co-authors' Analytic Cluster Model.

S2.1 Considerations regarding the Analytic Cluster Model and the determination of several properties of isolated Pt clusters/ nanoparticles

Parr and Pearson[8-10] have shown that the negative of the electron chemical potential μ in the density functional theory (DFT),[10] which is a fundamental property of a considered system (atom, molecule, ion, radical) in its ground state, is identical to χ, its electronegativity:

$$-\mu = (\frac{\partial E}{\partial N})_v = \chi \quad \text{(S7)}$$

where $(\frac{\partial E}{\partial N})_v$ is the partial derivative of the energy, E, of a system (DFT considers atom, molecule, ion, radical as a system of nuclei and electrons) with respect to the number of electrons N at a constant external potential, v, (nuclear-electron type). It was shown[8,9] that the chemical potential μ (or the "absolute" electronegativity) for an isolated atom A can be calculated using the first ionization potential, IP_A, and the electron affinity, EA_A, of the atom A, as follows:

$$-\mu_A(\text{eV}) = \chi_A = (IP_A + EA_A)/2 \quad \text{(S8)}$$

In application to clusters/nanoparticles of n platinum atoms, Pt_n, we believe that, since the chemical potential within the framework of the density functional theory is defined at each point and any region of the space, the following equation should be valid to assess the electronegativity of a Pt cluster or a Pt nanoparticle:

$$-\mu_{Pt_n}(eV) = \chi_{Pt_n} = (IP_{Pt_n} + EA_{Pt_n})/2 \quad \text{(S9)}$$

where IP_{Pt_n} and EA_{Pt_n} are the ionization potential and the electron affinity of a Pt cluster/nanoparticle.

To determine these quantities, we resorted to the Analytic Cluster Model of Müller and co-authors.[11] According to these authors, the property, G(n), of M_n clusters that may either be, its ionization potential, its electron affinity, or its cohesive or binding energy may be described using the first two terms of the following expansion:

$$G(n) = c_0 + c_{-1}/n^{1/3} \quad \text{(S10)}$$

where n is the number of atoms in a cluster (a parameter involved in the cluster size);

$$c_0 = G(\infty); \text{ (i.e., } c_0 \text{ is the bulk value of } G) \quad \text{(S11)}$$

$$c_{-1} = c_{-1}(n) = [G(n) - G(\infty)]n^{1/3}; n = 1,2,3, \ldots \quad \text{(S12)}$$

The application of these formulae requires only knowing: i) the bulk value $G(\infty)$ tabulated for many properties in the literature and ii) the value of $G(n)$ for a cluster containing n atoms. Since $G(n)$ value should be measured or calculated for some selected value of n, it means that one needs only one measurement to get information on the convergence of $G(n)$ on the whole region of n = 1, …, ∞.

S2.2 Determination of the cohesive (binding) energy of Pt cluster/nanoparticle

In accordance with the Analytic Cluster Model,[11] introduced above, we can write:

$$BE^{Pt}(n) = BE^{Pt}_{bulk} + 2^{1/3}(½D_e - BE^{Pt}_{bulk})/n^{1/3} \quad \text{(S13)}$$

where BE_{bulk}^{Pt} is the binding energy per atom of bulk Pt (numerically equal to the enthalpy of atomization) and D_e is the binding energy of the Pt-dimer (Pt_2) equals to the bond dissociation energy, and n is the number of atoms in a cluster. Substituting the values of BE_{bulk}^{Pt} = 5.86 eV[12] (1eV = 96.485 kJ mol^{-1}) and D_e = 3.178 eV[12] into eq S13, leads to the following relationship:

$$\boldsymbol{BE^{Pt}(n) = 5.86 - 5.38/n^{1/3}} \quad \text{(S14)}$$

The values obtained applying eq S14 are in fairly good agreement with DFT data reported in refs 2 and 13. For example, using eq S14, the BE^{Pt} = 2.71 eV is obtained for five-atomic Pt-cluster (in comparison with the DFT-derived value of 2.784 eV[2]) and for a nanoparticle of Pt of the size of 1.4 nm (for which the n value corresponds to ~56 atoms; eqs S1 or S4), BE^{Pt} = 4.45 eV.

S2.3 Determination of the ionization potential (IP) of Pt cluster/nanoparticle

The equation for the determination of the ionization potentials for Pt_n-clusters has the following form:[11]

$$IP^{Pt}(n) = \phi_{bulk}^{Pt} + (IP^{Pt} - \phi_{bulk}^{Pt})/n^{1/3} \quad \text{(S15)}$$

where ϕ_{bulk}^{Pt} is the work function of the platinum metal (6.35 eV[14]) and IP^{Pt} is the first ionization potential of Pt-atoms (8.9587 eV).[12] Thus, the ionization potential of Pt-clusters/nanoparticles is approximated by:

$$\boldsymbol{IP^{Pt}(n) = 6.35 + 2.61/n^{1/3}} \quad \text{(S16)}$$

S2.4 Determination of the electron affinity (EA) of Pt cluster/nanoparticle

The information about the values of electron affinity of Pt-clusters from different sources (mostly as results of DFT calculations) are very scattered.[13, 15-17] The accessible information was treated using the graph of the type: EA^{Pt} versus $n^{-1/3}$. From the graph (which is not given here), the following equation, which can predict the electron affinity of Pt-clusters, was obtained:

$$\boldsymbol{EA^{Pt}(n) \approx 5.26 - 4.50/n^{1/3}} \quad \text{(S17)}$$

We note that the value of c_0 = 5.26 eV in eq S17 is close to the Fermi level for bulk platinum (5.32 eV).[14] The Fermi level of a solid-state body is, by definition, the thermodynamic work required to add one electron to the body.[18] Calculated values of $EA^{Pt}(n)$ for Pt_2-Pt_5 clusters by using eq S17 are in a satisfactory agreement with the experimental data of different authors cited in ref 13.

S2.5 Determination of the energy value of the Pt-Pt bond of Pt cluster/nanoparticle

The E_{Pt-Pt} value in a cluster/nanoparticle of platinum, can be determined using the relation between the enthalpy of atomization of a cluster or nanoparticle and the coordination number of Pt atoms. In our case, this role is played by the mean coordination number, $\overline{CN}$ (see Section S1.2 of SI). The mean coordination number is defined as the quotient of the total number of pairwise nearest neighbors divided by the number of atoms.[6] Thus, the equation for E_{Pt-Pt} has the following form:

$$\boldsymbol{E_{Pt-Pt} = 2\Delta H_{at}^{Pt_n}/\overline{CN}} \quad \text{(S18)}$$

where $\Delta H_{at}^{Pt_n}$ is the enthalpy of atomization of the Pt_n-particle, which is numerically equal to its cohesive (binding) energy: $BE^{Pt}(n)$. Note that the derivation of the equation to determine the cohesive or the binding energy ($BE^{Pt}(n) = 5.86 - 5.38/n^{1/3}$) of Pt clusters/nanoparticles is given in Section S2 of SI. The correlation equations between the number of Pt-atoms in clusters and nanoparticles and the mean coordination number ($\overline{CN}$)are given in Section S1.2.

The calculated values of $IP^{Pt}(n)$, $EA^{Pt}(n)$, χ_{Pt_n} and E_{Pt-Pt} for Pt_n several metal clusters/nanoparticles are listed in Table 1 of the main text.

S2.6 Illustrative calculation of the adsorption energy for Pt_{30} cluster and results of some calculations of the adsorption energy using data from Table 1 of the main text.

i) the formation energy of a Pt_{30} cluster is: $BE_{Pt_{30}} \times 30 = -4.13 \times 30 = -123.9$ eV.

ii) the number of Pt-Pt bonds in Pt_{30} cluster is: the formation energy of a Pt_{30} cluster/$E_{Pt-Pt}^{Pt_{30}} = 123.9/1.40 = 88$.

iii) the reciprocal mean value of 1.64 and 1.40 eV is: $(2 \times 1.64 \times 1.40)/(1.64+1.40) = 1.51$ eV; where 1.64 eV is the mean value of $E_{Pt-Pt}^{Pt_n}$ for n comprised between 4 and 19, and 1.40 is $E_{Pt-Pt}^{Pt_n}$ for Pt_{30} .

iv) the formation energy of the graphene/Pt_{30} complex is calculated being equal to -[(3 × Pt-C bond energy) + (3 × Pt-Pt reciprocal mean energy) plus the energy of the cluster residue (or 88-3 times $E_{Pt-Pt}^{Pt_{30}}$)] = -(3×2.51 +3×1.51 + 85×1.40) = -131.06 eV.

v) the adsorption energy of the Pt_{30} cluster is: the formation energy of the graphene/Pt_{30} complex minus the formation energy of the Pt_{30} cluster is: -131.06 - (-123.9) = -7.16 eV.

S3. Determination of the electronegativity of non-doped and N-doped carbon substrates using their work functions.

Since the atoms of carbon substrates form a system of π-conjugated C-C bonds, it means that, in the calculations related to the present work, it is possible to operate with the electronegativity of graphene or that of any other carbon substrates, rather than with the electronegativity of carbon atoms. For example, using the pristine graphite's work function value (ϕ = 4.62 eV)[19] into eq S19

$$\chi = 0.50\phi - 0.29 \quad \text{(S19)}$$

which describes the behavior of semi-metals[20] (graphite can be considered as a semi-metal), one obtains that $\boldsymbol{\chi = 2.02}$ **eV$^{1/2}$ for the electronegativity of carbon substrates** (in Pauling scale of electronegativity), comparing with the electronegativity χ = 2.55 eV$^{1/2}$ of carbon atoms. When the carbon substrate is N-doped, it is important to note that the work function of graphene and graphite correlates strongly with their amount of doped nitrogen.[21-23] Nitrogen atoms doped at graphitic sites lower the work function, while nitrogen atoms located at pyridinic or pyrrolic sites increase the work function.[21-23] For instance, the N-plasma doped highly oriented pyrolytic graphite (treated with a hydrogen plasma during 5 minutes), for which N atoms substitute for graphitic C atoms,

exhibits a work function value of ϕ = 2.9 eV.[21] Substituting this value (which is in line with the work functions of alkaline earth metals) into eq S20, which is another correlation describing the behavior of these metals,[20]

$$\chi = 0.23\phi + 0.36 \quad \text{(S20)}$$

gives χ **= 1.03 eV$^{1/2}$ for the electronegativity of** (H-plasma treated) **N-doped graphite**, a value close to the electronegativity of calcium atoms.

S4. Determination of the bond energy value of Pt-C and Pt-N using the modification of the Matcha equation

Concerning the determination of the Pt-C bond energy, E_{Pt-C}, this value can be evaluated using the following equation,[24,25] which is a modification of the Matcha's equation:[26]

$$E_{Pt-C}(kJmol^{-1}) = (E_{Pt-Pt}E_{C-C})^{1/2} + 160[1 - e^{-0.29(\chi_{Pt_n}-\chi_{C_m})^2}] \quad \text{(S21)}$$

In eq S21, the first and second terms represent the covalent and ionic contributions to Pt-C bond energy, respectively; E_{Pt-Pt} and E_{C-C} are the energies of ordinary Pt-Pt and C-C bonds, and χ_{Pt_n} and χ_{C_m} are the electronegativities (in Pauling's scale of electronegativity) of the Pt-cluster/nanoparticle and carbon substrate, respectively. Considering an A-B bond, the Matcha's equation has the following form:

$$D_{AB}\ (\text{kcal mol}^{-1}) = D_{AB}^{cov} + K[1 - \exp\{-30(\Delta\chi)^2\}/K] \quad \text{(S22)}$$

where the first and the second terms refer to the covalent and ionic contributions into the energy of the A-B bond, respectively, and $\Delta\chi$ refers to the electronegativity difference $\chi_A - \chi_B$. The covalent term D_{AB}^{cov} is equal to the geometric mean $(D_{AA}D_{BB})^{½}$ of ordinary A-A and B-B bonds. Finally, K= 103. Matcha notes that predicted bond energies are found to vary from measured ones by an average of about 3%.[26]

To assess Pt-N bond energy, eq S23 (similar to eq S21) can be applied:

$$E_{Pt-N}(kJmol^{-1}) = (E_{Pt-Pt}E_{N-N})^{1/2} + 160[1 - e^{-0.29(\chi_{Pt_n}-\chi_{N/C_m})^2}] \quad \text{(S23)}$$

where the first and second terms represent the covalent and ionic contributions into the Pt-N bond energy, respectively; E_{Pt-Pt} and E_{N-N} are the energies of ordinary Pt-Pt and N-N bonds; and χ_{Pt} and χ_{N/C_m} are the electronegativities of the Pt_n cluster and the N-doped graphene, respectively.

S5. Sanderson-Boudreaux model of polar covalence for the calculation of partial charges on atoms and bonds energy

As can be seen from eq S7, the chemical potential (the "absolute" electronegativity) is linked to the energy required for charging an atom in a molecule. As it was shown by Pearson,[8,9] the energy, $(\frac{\partial E}{\partial N})_v$, governs the charge transfer in the process of a molecule formation. Consequently, it becomes possible to determine the ionicity of a chemical bond as well as the ionic contribution to the bond energy. As far as the corresponding covalent contribution to the bond

energy is concerned, it is usually determined as an arithmetic or geometric mean of the associated homonuclear ordinary bond energy.[27] Here, the most successful and consistent approach was developed by Sanderson.[28] According to Sanderson, the energy of the A-B bond in a given molecule can be evaluated by the following sum of an ionic and a covalent contribution:

$$E(kJ\ mol^{-1}) = t_i \frac{1389}{d_{A-B}} + (1 - t_i) \frac{(r_A + r_B)}{d_{A-B}} (E_{A-A} E_{B-B})^{½} \quad \text{(S24)}$$

where the first and second members in eq S24 refer to the ionic and covalent contributions into the A-B bond energy, respectively; t_i is the ionic weighting coefficient; d_{A-B} is the interatomic distance; r_A and r_B are the covalent radii of atoms A and B; and E_{A-A} and E_{B-B} are the homonuclear single covalent bond energies. The ionic weighting coefficient, t_i, is calculated as follows:

$$t_i = (q_A - q_B)/2 \quad \text{(S25)}$$

where q_A and q_B are the partial charges on the atoms A and B. The partial charge on the atom A is given by

$$q_A = \frac{\chi_M - \chi_A^o}{1.57\sqrt{\chi_A^o}} \quad \text{(S26)}$$

where χ_M is the equalized electronegativity of the molecule. An analogous equation is valid for the atom B. For a molecule consisting of n atoms, the equalized electronegativity is:

$$\chi_M = (\prod_i^n \chi_i^o)^{1/n} \quad \text{(S27)}$$

where χ_i^o, is the electronegativity of the i_{th} isolated atom.

Eq S26 has been modified by Boudreaux[29] to eq S28, which considers the total number of atoms, n_T, bound to a given atom A, since **the partial charge on atom A, q_A,** varies, accordingly to his opinion, in proportion to the numbers of atoms bound to it as follows:

$$\boldsymbol{q_A = \frac{1}{3.12 n_T \sqrt{\chi_A}} [(\chi_M - \chi_A) + \sum(\chi_{n_i} - \chi_A)]} \quad \text{(S28)}$$

where χ_{n_i} is the electronegativity of each n_{th} atom, and χ_M is also calculated, according to eq S27 as the geometrical mean of the electronegativity of all atoms composing the molecule. The fractional ionic character of the atom A bound to n atoms is:

$$\boldsymbol{t_i(A) = \frac{|q_A - \sum n q_n|}{1+n}} \quad \text{(S29)}$$

In the basic Sanderson method, the equalized electronegativity, χ_M, (eq S27), does not contain the connectivity information and, thus, does not account for different electronegativities for the same atom in different environments. For example, the calculation of χ_M does not differentiate between the hydrogen atoms in a molecule of acetic acid where these atoms have a different functionality. To solve this problem, Gray and Hercules[30] modified the original Sanderson method. They proposed to use in the calculation of the equalized electronegativity of a molecule, the χ_M values

of chemical groups, χ_g, composing the molecule, instead of the electronegativity of isolated atoms. In this case, a molecule is considered as a central atom directly bound to the chemical groups. A chemical group is defined as any atom or group of atoms bound to the atom of interest. In turn, the equalized electronegativity of a group is calculated (eq S27), using the tabulated electronegativities of atoms composing this group. In the case of the CH_3COOH molecule, for instance, the charge on the carbon atom of the carboxyl group would be calculated (eq S28) using

$$\chi_M = \sqrt[4]{\chi_C \chi_{CH_3} \chi_O \chi_{OH}} \quad \text{(S30)}$$

where χ_C and χ_O are tabulated electronegativities, and χ_{CH_3} and χ_{OH} are calculated by eq S27.

A knowledge of the partial charges depending on the environment first enables the determination of the ionic weighting coefficient, t_i, (eq S29). Then, having the information about the interatomic distances and covalent radii of the atoms, the calculation of the bond energy of interest in this work (Pt-C and Mn-N bonds) becomes possible (eq S24). Therefore, it seems possible (Section 2.3 and Section 3) to estimate the binding energy (as a measure of the adhesion strength) of Pt clusters/nanoparticles to graphene substrates either in the presence or in absence of integrated MnN_x/C sites into graphene. Finally, using the obtained values of Mn-N bond energy, we will also be able to assess the equilibrium constants of demetallation reactions (manganese acid leaching) of the MnN_x/C sites in the hybrid Pt_n-MnN_x/C electrocatalysts, as a criterium of chemical stability of the hybrid sites in PEM fuel cells, (Section 4).

S6. Illustrative calculations of charge distribution on atoms, and Pt-C and Mn-N bond energies in the modelled hybrid Pt_2-$Mn^{III}N_4$/C site of Figure 3a of the main text.

The electronegativity of Pt_2 (Figure 3a of the main text), as a chemical group, $\chi_g(Pt_2)$, was taken, following the Sanderson principle of the full equalization, equal to $\sqrt{\chi_{Pt} \times \chi_{Pt}}$, i.e., to the same of Pt atom's electronegativity. It applies equally to the determination of χ_g for a graphene lattice. Thus, the value of χ_g of the Pt_2 cluster, forming three bonds with carbon atoms of graphene, is equal (using the data of Table 5 of the main text) to

$$\chi_g(Pt_2C_{m=3}) = \sqrt[4]{2.14 \times 2.746^3} = 2.580.$$

For the $Mn^{(III)}N_4$ group interacting with eight carbon atoms, it is:

$$\chi_g(MnN_4C_{m=8}) = \sqrt[13]{2.20 \times 3.194^4 \times 2.746^8} = 2.828.$$

The equalized electronegativity of the site is:

$$\chi_M = \sqrt{2.580 \times 2.828} = 2.701.$$

The charge on Pt atom, q_{Pt}, is, eq S28:

$$q_{Pt} = \frac{1}{3.12 \times 3 \times \sqrt{2.14}} [(2.701 - 2.14) + 3 \times (2.746 - 2.14)] = +0.174.$$

The charge on the carbon atom in the chain Pt-C-N, considering that this atom forms one bond each with Pt, N and C (Figure 3a), is:

q_C (Pt-C-N) $= \frac{1}{3.12\times3\times\sqrt{2.746}}[(2.701-2.746)+(2.14-2.746)+(3.194-2.746)] =$ -0.013.

The charge on the carbon atom, considering that each atom of C forms one bond with Pt and two bonds with C atoms (Figure 3a), is:

$q_C = \frac{1}{3.12\times3\times\sqrt{2.746}}[(2.701-2.746)+(2.14-2.746)]$ = -0.042.

The fractional ionic character of the Pt atom, bound to a single graphene vacancy, eq S29, is:

t_i(Pt) = $\frac{|0.174-(-0.013)-2(-0.042)|}{1+3}$ = 0.068.

Let's estimate the Pt-C interatomic distance using the well-known Shoemaker-Stevenson's formula:[31]

$$d_{AB} = r_A + r_B - 0.09 \mid \Delta\chi_{AB} \mid$$

where r_A and r_B are the covalent radii of atoms A and B, $\Delta\chi_{AB}$ is the difference of the electronegativities of A and B atoms (in Pauling scale electronegativity). We obtain:

d_{PtC} = 1.37 + 0.772 – 0.09|1.69-2.55| = 2.07 Å ≅ 2.1 Å.

Using eq S24, we obtain:

$E_{Pt-C} = 0.068\frac{1389}{2.1} + (1-0.068)\frac{(1.37+0.772)}{2.1}(158.2\times357.3)^{½}$ = 270.8 kJ mol^{-1} = 2.81 eV.

Comparing the obtained value with the Pt-C bond energy of 2.51 eV (Section 2.2), it can be seen that the $Mn^{III}N_4$ grouping, integrated into a graphene lattice, noticeably (at 0.29 eV) strengthens this bond. The adsorption (binding) energy of Pt_2 cluster is (Sections 2.1 and 2.2): -(3×2.81+ 1×1.64 – 3.18) = -6.89 eV, that is more than the value of -5.99 eV (Table 2).

The charge on the Mn atom of the $(MnN_4C_{m=8})$ grouping is:

$q_{Mn} = \frac{1}{3.12\times4\times\sqrt{2.20}}[(2.701-2.20)+4\times(3.194-2.20)]$ = +0.242.

The charge on N atoms (coordinated to Mn), considering that each atom of N forms one bond with Mn and two bonds with C atoms (Figure 3a), is:

$q_N = \frac{1}{3.12\times3\times\sqrt{3.194}}[(2.701-3.194)+2\times(2.746-3.194)+(2.20-3.194)]$ = -0142.

The fractional ionic character of Mn atom, eq S29, is:

t_i(Mn) = $\frac{|0.242-4(-0.142)|}{1+4}$ = 0.162.

The value of Mn-N bond energy (eq S24) is:

$E_{Mn-N} = 0.162\frac{1389}{2.0} + (1-0.162)\frac{(1.28+0.734)}{2.0}[(121.0\pm29)\times156.3)]^{½}$ = 227.7±14 kJ mol^{-1}.

The obtained value, comparing with the values in the range from 215.8 to 219.7 kJ mol^{-1} for MnN_4 grouping integrated into graphene,[32] is reasonable, considering that the hybridization of two sites

mutually enhances the strength of Pt-C and Mn-N bonds. The value of 2.0 Å was taken from ref 32.

Note that in this work, calculations of the energetics of adsorption and chemical bonds were performed based on the modern concept of electronegativity. Pearson,[8,9] and Parr and Yang,[10] gave a precise definition of the electronegativity (eq S7), which was known and successfully used for many years in various branches of chemistry for the calculations of partial charges on atoms and bonds energy in molecules and solids, using the electronegativity equalization principle formulated by Sanderson.[28] This principle states that "when two or more atoms initially different in electronegativity chemically combine, their electronegativities equalize in the molecule". The validity of Sanderson's principle is due to the fact that the electronic chemical potential μ (or the "absolute" electronegativity) is the property of an equilibrium state.[10] Sanderson in his monograph[28] notes that the validity of partial charges determined using this principle have been proven in the accurate calculations of energies of about 15000 bonds between more than 200 different pairs.

Figures.

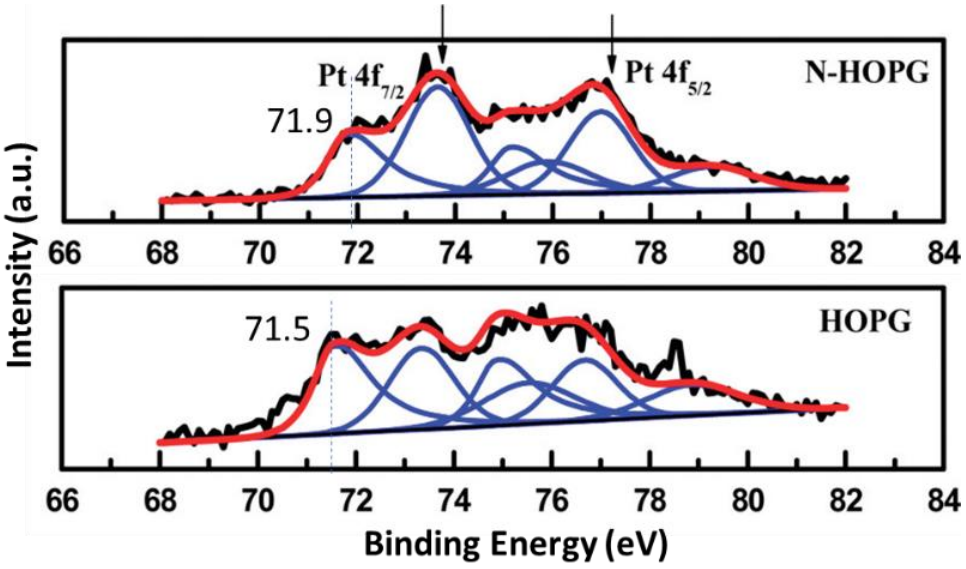

Figure S1: Comparison of the Pt 4f core level XPS of Pt nanoparticles on undoped (HOPG), and N-doped HOPG substrates.
Black line: original curve; Red line: fitting curve; Blue line: deconvolution curve.
Reproduced from ref 33.

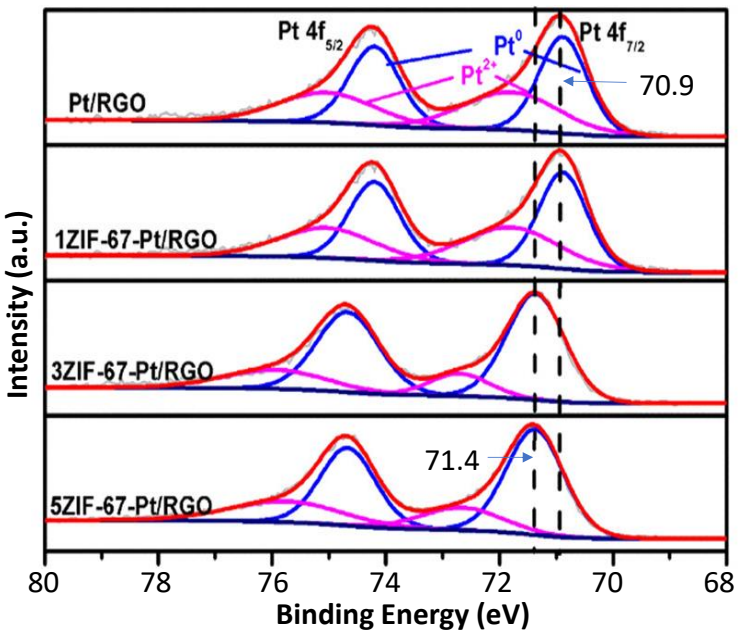

Figure S2: XPS Pt 4f spectra of Pt/RGO and Pt/RGO with different cycles of ZIF-67. Reproduced from ref 34.

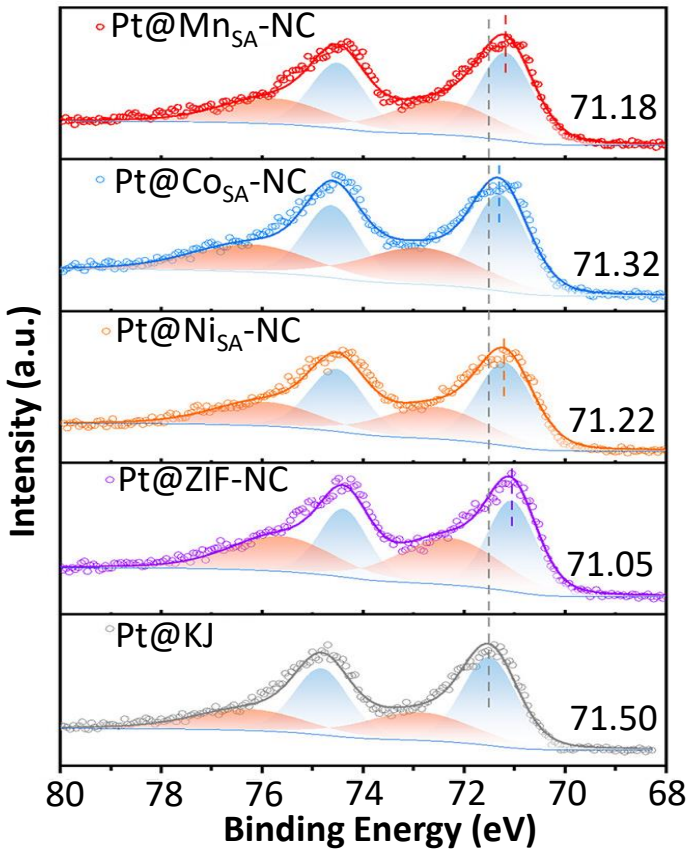

Figure S3: Pt 4f XPS of the Pt catalysts supported on ZIF-NC and KJ (Ketjen Black), in which Pt@Ketjen Black and Pt@ZIF-NC served as the baseline. Reproduced from ref 35.

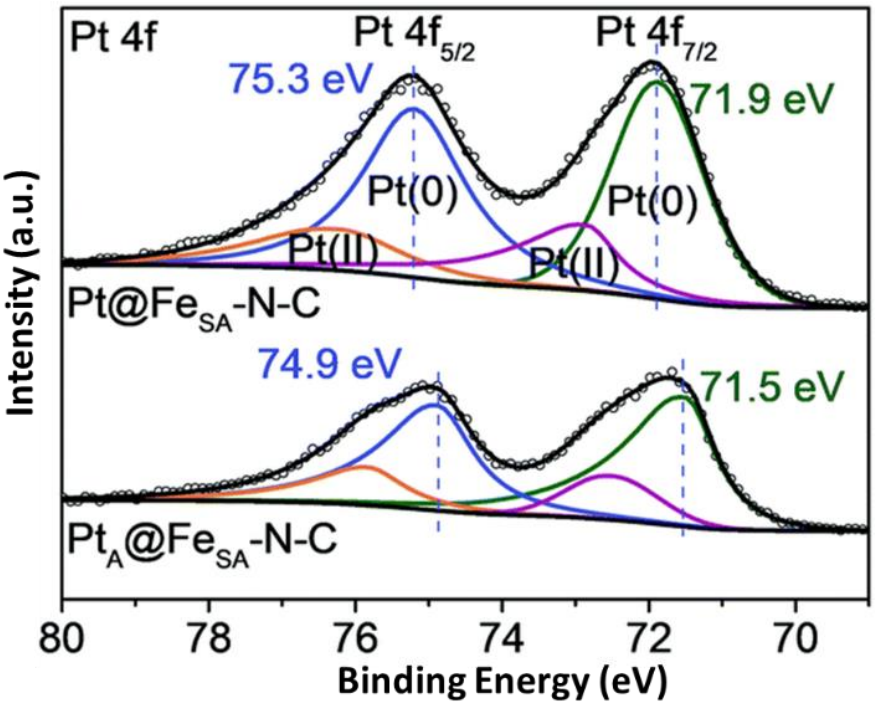

Figure S4: XPS spectra of Pt 4f for Pt@Fe_{SA}-N-C and Pt_A@Fe_{SA}-N-C. Reproduced from ref 36.

References to Supporting Information

1. Wong, K.; Vongehr, S.; Kresin, V. V., Work functions, ionization potentials, and in between: Scaling relations based on the image-charge model. *Phys. Rev. B* **2003,** *67* (3), 035406. DOI: 10.1103/PhysRevB.67.035406
2. Nie, A.; Wu, J.; Zhou, C.; Yao, S.; Luo, C.; Forrey, R. C.; Cheng, H., Structural evolution of subnano platinum clusters. *Int. J. Quantum Chem.* **2007,** *107* (1), 219-224. DOI: 10.1002/qua.21011
3. Poidevin, C.; Paciok, P.; Heggen, M.; Auer, A. A., High resolution transmission electron microscopy and electronic structure theory investigation of platinum nanoparticles on carbon black. *J Chem Phys* **2019,** *150* (4), 041705. DOI: 10.1063/1.5047666
4. Qureshi, M.; Garcia-Esparza, A. T.; Jeantelot, G.; Ould-Chikh, S.; Aguilar-Tapia, A.; Hazemann, J.-L.; Basset, J.-M.; Loffreda, D.; Bahers, T. L.; Takanabe, K., Catalytic consequences of ultrafine Pt clusters supported on SrTiO3 for photocatalytic overall water splitting. *Journal of Catalysis* **2019,** *376*, 180-190. DOI: 10.1016/j.jcat.2019.06.045
5. Miracle, D. B.; Senkov, O. N., A critical review of high entropy alloys and related concepts. *Acta Materialia* **2017,** *122*, 448-511. DOI: 10.1016/j.actamat.2016.08.081

6. Benfield, R. E., Mean coordination numbers and the non-metal–metal transition in clusters. *J. Chem. Soc., Faraday Trans.* **1992,** *88* (8), 1107-1110. DOI: 10.1039/ft9928801107
7. Wei, G. F.; Liu, Z. P., Subnano Pt Particles from a First-Principles Stochastic Surface Walking Global Search. *J Chem Theory Comput* **2016,** *12* (9), 4698-4706. DOI: 10.1021/acs.jctc.6b00556
8. Pearson, R. G., Absolute electronegativity and absolute hardness of Lewis acids and bases. *Journal of the American Chemical Society* **1985,** *107* (24), 6801-6806. DOI: 10.1021/ja00310a009
9. Pearson, R. G., Chemical hardness and density functional theory. *Journal of Chemical Sciences* **2005,** *117* (5), 369-377. DOI: 10.1007/bf02708340.
10. Parr, R. G.; Yang. W., *Density-Functional Theory of Atoms and Molecules*. Oxford University Press; Clarendon Press: New York: New York: Oxford, 1989.
11. Müller, H.; Fritsche, H.-G.; Scala, L., Analytic Cluster Models and Interpolation Formulae for Clusters Properties. In *Clusters of Atoms and Molecules: Theory, Experiment, and Clusters of Atoms*, Haberland, H., Ed. Berlin–Heidelberg, 1995; Vol. 52.
12. *CRC Handbook of Chemistry and Physics, 96th Edition*. CRC Press: Taylor and Francis Group: Boca Raton, Fl, 2015-2016.
13. Singh, N. B.; Sarkar, U., Structure, vibrational, and optical properties of platinum cluster: a density functional theory approach. *J Mol Model* **2014,** *20* (12), 2537. DOI: 10.1007/s00894-014-2537-5
14. Bordoloi, A. K.; Auluck, S., Electronic structure of platinum. *Journal of Physics F: Metal Physics* **1983,** *13*, 2101-2105. DOI: 10.1088/0305-4608/13/10/019
15. Yang, S. H.; Drabold, D. A.; Adams, J. B.; Ordejón, P.; Glassford, K., Density functional studies of small platinum clusters. *Journal of Physics: Condensed Matter* **1997,** *9* (5), L39-L45. DOI: 10.1088/0953-8984/9/5/002
16. Chen, Z.; Msezane, A. Z. Electron affinity of small Pt clusters. In American Physical Society, 41st Annual Meeting of the APS Division of Atomic, Molecular and Optical Physics *(Bulletin of the American Physical Society 2010)*, Houston, Texas; BAPS.2010.DAMOP.E1.174
17. Grönbeck, H.; Andreoni, W., Gold and platinum microclusters and their anions: comparison of structural and electronic properties. *Chemical Physics* **2000,** *262* (2), 1-14. DOI: 10.1016/S0301-0104(00)00294-9
18. Kittel, C., *Introduction to Solid State Physics*. 2nd ed.; John Wiley and Sons: U.S., 1956.
19. Jain, S.C.; Srinivasta, K.K., The thermionic constants of metals and semi-conductors I. Graphite. *Proceedings of the Royal Society of London. Series A. Mathematical and Physical Sciences* **1952,** *213* (1113), 143-157. DOI: 10.1098/rspa.1952.0116
20. Trasatti, S. Electronegativity, work function, and heat of adsorption of hydrogen on metals. *Journal of the Chemical Society, Faraday Transactions 1: Physical Chemistry in Condensed Phases* **1972,** *68*, 229-236. DOI: 10.1039/f19726800229
21. Schiros, T.; Nordlund, D.; Palova, L.; Prezzi, D.; Zhao, L.; Kim, K. S.; Wurstbauer, U.; Gutierrez, C.; Delongchamp, D.; Jaye, C.; Fischer, D.; Ogasawara, H.; Pettersson, L. G.; Reichman, D. R.; Kim, P.; Hybertsen, M. S.; Pasupathy, A. N., Connecting dopant bond type with electronic structure in N-doped graphene. *Nano Lett* **2012,** *12* (8), 4025-31. DOI: 10.1021/nl301409h
22. Akada, K.; Obata, S.; Saiki, K., Work Function Lowering of Graphite by Sequential Surface Modifications: Nitrogen and Hydrogen Plasma Treatment. *ACS Omega* **2019,** *4* (15), 16531-16535. DOI: 10.1021/acsomega.9b02208.

23. Akada, K.; Terasawa, T.; Imamura, G.; Obata, S.; Saiki, K., Control of work function of graphene by plasma assisted nitrogen doping. *Applied Physics Letters* **2014,** *104* (13) 131602. DOI: 10.1063/1.4870424.
24. Shnyp, V. A.; Glibin, V.P; Poplavski, V. V., Binding energy of surface complexes and catalytic activity of some metals in the reaction of CO oxidation. *Bulletin of Belarussian Academy of Sciences. Chemical Section* **1994,** *4*, 76-80. (in Russian)
25. Glibin, V.; Svirko, L.; Lynkov, L.; Gurov, A.; Petrov, N.; Zakharov, V.; Boldysheva, I., On the problem of evaluating adhesion of oxide coatings on metals. In *Physics, Chemistry and Application of Nanostructures: Review and Short Notes to Nanomeeting'97*, Word Scientific Publishing Co. Pte. Ltd.: Singapoore, 1997; pp 159-162.
26. Matcha, R. L., Theory of the chemical bond. 6. Accurate relationship between bond energies and electronegativity differences. *Journal of the American Chemical Society* **1983,** *105* (15), 4859-4862. DOI: 10.1021/ja00353a002.
27. Pauling, L., *The Nature of the Chemical Bond*. 3rd ed.; Cornell University Press: Ithaca; New York, 1960.
28. Sanderson, R. T., *Polar Covalence*. Academic Press New York: London; Toronto, 1983.
29. Boudreaux, E. A., Calculations of bond dissociation energies. New select applications of an old method. *J Phys Chem A* **2011,** *115* (9), 1713-20. DOI: 10.1021/jp108920e.
30. Gray, R. C.; Hercules, D. M., Correlations between ESCA chemical shifts and modified sanderson electronegativity calculations. *Journal of Electron Spectroscopy and Related Phenomena* **1977,** *12* (1), 37-53. DOI: 10.1016/0368-2048(77)85066-4.
31. Schoemaker, V.; Stevenson, D. P., Some Revisions of the Covalent Radii and the Additivity Rule for the Lengths of Partially Ionic Single Covalent Bonds. *Journal of the American Chemical Society* **1941,** *63* (1), 37-40. DOI: 10.1021/ja01846a007.
32. Glibin, V. P.; Dodelet, J.-P.; Zhang, G., Spontaneous Demetallation of Mn(II)Nx Catalytic Sites in Proton Exchange Membrane Fuel Cell Conditions. *ACS Catalysis* **2024,** *14* (1), 330-343. DOI: 10.1021/acscatal.3c04310.
33. Zhou, Y.; Holme, T.; Berry, J.; Ohno, T. R.; Ginley, D.; O'Hayre, R., Dopant-Induced Electronic Structure Modification of HOPG Surfaces: Implications for High Activity Fuel Cell Catalysts. *The Journal of Physical Chemistry C* **2010,** *114* (1), 506-515. DOI: 10.1021/jp9088386
34. Wu, W.; Zhang, Z.; Lei, Z.; Wang, X.; Tan, Y.; Cheng, N.; Sun, X., Encapsulating Pt Nanoparticles inside a Derived Two-Dimensional Metal-Organic Frameworks for the Enhancement of Catalytic Activity. *ACS Appl Mater Interfaces* **2020,** *12* (9), 10359-10368. DOI: 10.1021/acsami.9b20781.
35. Zeng, Y.; Liang, J.; Li, C.; Qiao, Z.; Li, B.; Hwang, S.; Kariuki, N. N.; Chang, C. W.; Wang, M.; Lyons, M.; Lee, S.; Feng, Z.; Wang, G.; Xie, J.; Cullen, D. A.; Myers, D. J.; Wu, G., Regulating Catalytic Properties and Thermal Stability of Pt and PtCo Intermetallic Fuel-Cell Catalysts via Strong Coupling Effects between Single-Metal Site-Rich Carbon and Pt. *J Am Chem Soc* **2023,** *145* (32), 17643-17655. DOI: 10.1021/jacs.3c03345.
36. Ao, X.; Zhang, W.; Zhao, B.; Ding, Y.; Nam, G.; Soule, L.; Abdelhafiz, A.; Wang, C.; Liu, M., Atomically dispersed Fe–N–C decorated with Pt-alloy core–shell nanoparticles for improved activity and durability towards oxygen reduction. *Energy & Environmental Science* **2020,** *13* (9), 3032-3040. DOI: 10.1039/d0ee00832j.